Aquaculture 565 (2023) 739151

Contents lists available at ScienceDirect

Aquaculture

journal homepage: www.elsevier.com/locate/aquaculture

Knockout of microphthalmia-associated transcription factor (*mitf*) confers a red and yellow tilapia with few pigmented melanophores

Chenxu Wang [a], Thomas D. Kocher [b], Jinzhi Wu [a], Peng Li [a], Guangyuan Liang [a], Baoyue Lu [a], Jia Xu [a], Xiaoke Chen [a], Deshou Wang [a,*]

[a] Key Laboratory of Freshwater Fish Reproduction and Development (Ministry of Education), Key Laboratory of Aquatic Science of Chongqing, School of Life Sciences, Southwest University, Chongqing 400715, China
[b] Department of Biology, University of Maryland College Park, MD 20742, USA

ARTICLE INFO

Keywords:
Mitf genes
Melanophores
Erythrophores and xanthophores
Red and yellow body color
RPE pigmentation
CRISPR/Cas9 gene editing

ABSTRACT

As the most important genetic factor for melanophore differentiation and melanogenesis, *mitf* has been studied for over 30 years. The phenotypes of *mitf* mutants have also received continuous attention for nearly a century. Due to the third round of genome duplication, teleosts have two *mitf* genes. Mutation analysis demonstrates that *mitfa* plays an important role in zebrafish pigmentation. However, there have been no functional studies on body color regulation by *mitfb* or studies of *mitfa;mitfb* double mutants. In the present study, we mutated both *mitf* genes in tilapia using CRISPR/Cas9. Disruption of *mitfa* resulted in light yellow body color with weak gray vertical bars due to significantly reduced numbers of melanophores and increased sizes of xanthophores, while disruption of *mitfb* led to slight hypo-pigmentation. Double mutation of *mitfa* and *mitfb* resulted in dramatic hypo-pigmentation in trunk and fins due to loss of additional melanophores and increase in the number of iridophores compared to the single mutants, but had no influence on retinal pigment epithelium (RPE) pigmentation. The *mitfa*$^{-/-}$;*mitfb*$^{-/-}$ mutants were yellow with black spots at early juvenile stage (60 dpf), yellow-reddish at late juvenile stage (120 dpf) and red and yellow (including iris) at adult stage (180 dpf), due to increased erythrophores and enlarged xanthophores. Our results demonstrated that both *mitf* genes are important for body color formation in tilapia, but *mitfa* plays a more important role than *mitfb*. Additionally, by comparing the phenotypes of the *mitfa*$^{-/-}$;*mitfb*$^{-/-}$, *pmela*$^{-/-}$;*pmelb*$^{-/-}$ and *hps4*$^{-/-}$ mutants, we found that disruption of genes with different functions in different aspects of melanogenesis could lead to different body colors in tilapia. *Mitf* is the most important gene for melanophore differentiation and is probably also critical for differentiation of erythrophores, xanthophores and iridophores. To our knowledge, this is the first report showing that both *mitf* genes are involved in body color formation by loss of function study, and the first report showing that erythrophore numbers and xanthophore sizes were affected by *mitf*. Our research not only serves as a model for studying *mitf* function in tilapia and the closely related cichlids, but also provides new strategies for breeding red and yellow tilapia for aquaculture.

1. Introduction

Body color and pattern is of great significance for camouflage, mate choice and environmental adaptation in vertebrates (Hoekstra, 2006; Hubbard et al., 2010; Hofreiter and Schöneberg, 2010). Fish, amphibians and reptiles share the same six types of pigment cells (also known as chromatophores). They are melanophores, xanthophores, iridophores, leucophores, erythrophores and cyanophores (Fujii, 2000; Sköld et al., 2016; Salis et al., 2019).

The pigment cells are differentiated from pluripotent precursors in the neural crest (neural crest cells, NCCs) and migrate to their destinations (Fukamachi et al., 2004; Lopes et al., 2008; Kimura et al., 2014). Many genes, including *mitf*, are involved in pigment cell precursor migration and differentiation (Lister et al., 1999; Frohnhöfer et al.,

Abbreviations: mitf, microphthalmia-associated transcription factor; *pmel*, premelanosome protein; *hps4*, Hermansky-Pudlak syndrome 4 protein; CRISPR/Cas9, clustered regularly interspaced short palindromic repeats/CRISPR-associated protein 9; RPE, retinal pigment epithelium; NCCs, neural crest cells..

* Corresponding author.
E-mail address: wdeshou@swu.edu.cn (D. Wang).

https://doi.org/10.1016/j.aquaculture.2022.739151
Received 3 November 2022; Received in revised form 7 December 2022; Accepted 10 December 2022
Available online 11 December 2022

2013). *Mitf* plays the most fundamental and central role in NCCs-melanoblast-melanophore differentiation and melanogenesis pathway (Mort et al., 2015; Vachtenheim and Borovanský, 2010; Goding and Arnheiter, 2019). The specific roles of *mitf* in the survival and differentiation of pigment cells have been studied in humans (George et al., 2016), mice (Hodgkinson et al., 1993), dogs (Körberg et al., 2014), mink (*Neovison vison*) (Song et al., 2017), Peking ducks (Zhou et al., 2018), *Xenopus* (Kawasaki et al., 2008), and many other tetrapods. Many natural mutants in vertebrates display albinism or are white with black spots (Körberg et al., 2014; Song et al., 2017; Zhou et al., 2018). Due to the third round of genome duplication, teleosts have two *mitf* genes, *mitfa* and *mitfb* (Braasch et al., 2009; Lorin et al., 2018). Loss of function of *mitfa* and *mitfb* in zebrafish (Lane and Lister, 2012) and *mitfa* in fighting fish (Wang et al., 2021b) has been reported. Although *mitf* genes have been associated with melanophore survival and melanogenesis in medaka (Béjar et al., 2003; Li et al., 2014) and carp (Liu et al., 2016), until now there has been no report showing *mitfb* is critical for body color formation in teleosts.

Mutation of *mitf* in human, mouse and pig leads to albinism with white hair and non-pigmented retinal pigment epithelium (RPE) (Hodgkinson et al., 1993; Hou and Pavan, 2008; Cheli et al., 2010; George et al., 2016; Wang et al., 2015; Hai et al., 2017). In contrast, mutation of the *mitf* gene leads to complete white plumage while normal pigmented RPE in ducks (Zhou et al., 2018). Mutation of *mitf* genes led to complete white body, but no affects on RPE pigmentation in zebrafish (*mitfa*$^{-/-}$, *mitfb*$^{-/-}$ and *mitfa*$^{-/-}$;*mitfb*$^{-/-}$ mutants) and fighting fish (*mitfa*$^{-/-}$ mutants) (Lister et al., 1999; Wang et al., 2021b). It is important to know whether *mitf* mutation influence RPE pigmentation in other vertebrates, especially in fishes.

Mitf genes belong to the MiT family of basic helix-loop-helix leucine zipper (bHLH-ZIP)-containing transcription factors. Interestingly, *tfec* of the MiT family has been found to be a regulator of melanophore and iridophore shared pigment cell precursors, thus important for pigment cell lineage specification in zebrafish (Petratou et al., 2018; Lister et al., 2011). The *mitfa*$^{-/-}$ mutants of zebrafish are yellow-pink, free of melanophores, but have increased iridophores (Lister et al., 1999). Subsequently, *mitfa* has been found to be involved in iridophore differentiation by interacting with the iridophore lineage-specific genes (Petratou et al., 2018). *mitf* was found to be down-regulated in red/white skin compared with the black skin of red tilapia (a natural mutant) by skin transcriptome analysis, indicating *mitf* was probably fundamental for the red body color formation (Zhu et al.,2016; Jiang et al., 2022a). There are only three major types of pigment cells in zebrafish. Whether *mitf* genes are also responsible for cell lineage specification of other types of pigment cells, such as erythrophores and xanthophores in teleosts, is still unclear.

In our previous studies, we developed Nile tilapia as a model for studying teleosts color patterns by mutating dozens of color genes, including melanosome biosynthesis genes like *tyrb*, *pmel* and *hps4* (Wang et al., 2021a). In the present study, we mutated the most important melanophore differentiation and melanogenesis genes, *mitfa* and *mitfb*, and analyzed their phenotypes at different developmental stages. Both genes were found to be critical for tilapia body color formation, while neither was found to be linked with RPE pigmentation. Strikingly, the adult *mitfa*$^{-/-}$;*mitfb*$^{-/-}$ mutants showed strong red and yellow body color, different from the *tyrb*$^{-/-}$, *pmela*$^{-/-}$;*pmelb*$^{-/-}$ and *hps4*$^{-/-}$ mutants. Generally, our study not only provides an excellent model for studying *mitf* function in vertebrates, but also provide a new strategy for breeding red and yellow tilapia for aquaculture.

2. Materials and methods

2.1. Fish

The founder strain of Nile tilapia was obtained from Prof. Nagahama (Laboratory of Reproductive Biology, National Institute for Basic Biology, Okazaki, Japan). This strain has been in laboratory culture for >20 years, and is thus largely homozygous. Experimental tilapia were reared in recirculating aerated freshwater tanks and maintained at ambient temperature (27 °C) under a natural photoperiod. Prior to the experiments, the fish were kept in laboratory aquariums under 15:9 h light: dark conditions at temperature of 27 ± 1 °C for one week. The PMEL-disrupted golden tilapia (180 dpf) and HPS4-disrupted silver-white tilapia (180 dpf) we previously engineered (Wang et al., 2022a, 2022b) were used for comparative analysis on the pigmentary basis of the three classical melanogenesis genes' color mutants. All animal experiments conformed to the Guide for the Care and Use of Laboratory Animals and were approved by the Committee for Laboratory Animal Experimentation at Southwest University, China.

2.2. Disruption of tilapia mitf genes by CRISPR/Cas9 gene editing

Like zebrafish and medaka, tilapia has two *mitf* genes (Wang et al., 2021a; Jiang et al., 2022b). CRISPR/Cas9 was performed to knockout *mitfa* and *mitfb* (Gene ID 100534525 and 100,699,256, respectively) in tilapia as described previously (Wang et al., 2021a). gRNA targets in exon 3 of *mitfa* and exon 2 of *mitfb* were used to disrupt the *mitf* genes in tilapia. The sequences of gRNA targets were CCGGTCCTGGCAGCAGTGCACCC and CCTGCCATCAATGTCAGTGTCCC, in which CCG and CCT were used as the PAM regions (Fig. 1A-1C and 1G-1I). The guide RNA and Cas9 mRNA were co-injected into one-cell-stage embryos at a concentration of 150 and 500 ng/μL, respectively. About 400 fertilized eggs were used for gene editing and 100 for control. Twenty injected embryos were collected 72 h after injection. Genomic DNA was extracted from pooled control and injected embryos and used to access the mutations. DNA fragments spanning the target site for each gene were amplified using gene-specific primers (*mitfa*-Cas-F/R and *mitfb*-Cas-F/R) listed in Table S1.The mutated sequences were analyzed by restriction enzyme digestion with *FspE*I and *Tsp45*I and Sanger sequencing. The survival rate was nearly 95% after injection.

Heterozygous F1 offspring were obtained by mating F0 XY male founders with WT XX females. The F1 fish were genotyped by fin clip assay and the individuals with frame-shift mutations were selected. XY male and XX female siblings of F1 generation, carrying the same mutation, were mated to generate homozygous F2 mutants. A heteroduplex mobility assay identified the heterozygous *mitfa*$^{+/-}$, *mitfb*$^{+/-}$ and *mitfa*$^{+/-}$;*mitfb*$^{+/-}$ individuals as those possessing both heteroduplex and homo-duplex amplicons vs. the *mitfa*$^{+/-}$ and *mitfa*$^{-/-}$, *mitfb*$^{+/-}$ and *mitfb*$^{-/-}$, and *mitfa*$^{-/-}$;*mitfb*$^{-/-}$ individuals with only homo-duplex amplicons. Primer sequences (*mitfa*-page-F/R and *mitfb*-page-F/R) used for mutants screening were listed in Table S1. The *mitfa*$^{-/-}$, *mitfb*$^{-/-}$ and *mitfa*$^{-/-}$;*mitfb*$^{-/-}$ mutants were confirmed using restriction enzyme digestion and Sanger sequencing. The genetic sex of each fish was determined by genotyping using a sex-linked marker (marker 5) as described previously (Sun et al., 2014).

2.3. Image recording and pigment cell observation at different developmental stages

Embryonic and larvae fish at 4, 5, 7, 12 and 30 days post fertilization (dpf) and early juvenile stage at 60 dpf were shifted to an observation dish with clean water, photographed by Olympus SZX16 stereomicroscope (Olympus, Japan) under bright or transparent field with different magnification. The 30 dpf and 60 dpf fish were firstly anesthetized with tricaine methasulfonate (MS-222, Sigma-Aldrich, USA) before been shifted to an observation dish and photographed. The 90 dpf wild-type and mutant fish were shifted to the same 10 × 5 × 10 cm^3 glass water tanks separately, before being photographed with a Nikon D7000 digital camera (Nikon, Japan) against a blue background. ACDSee Official Edition software (ACDSystems, Canada) and Adobe Illustrator CS6 (Adobe Inc. USA) were used to format the pictures.

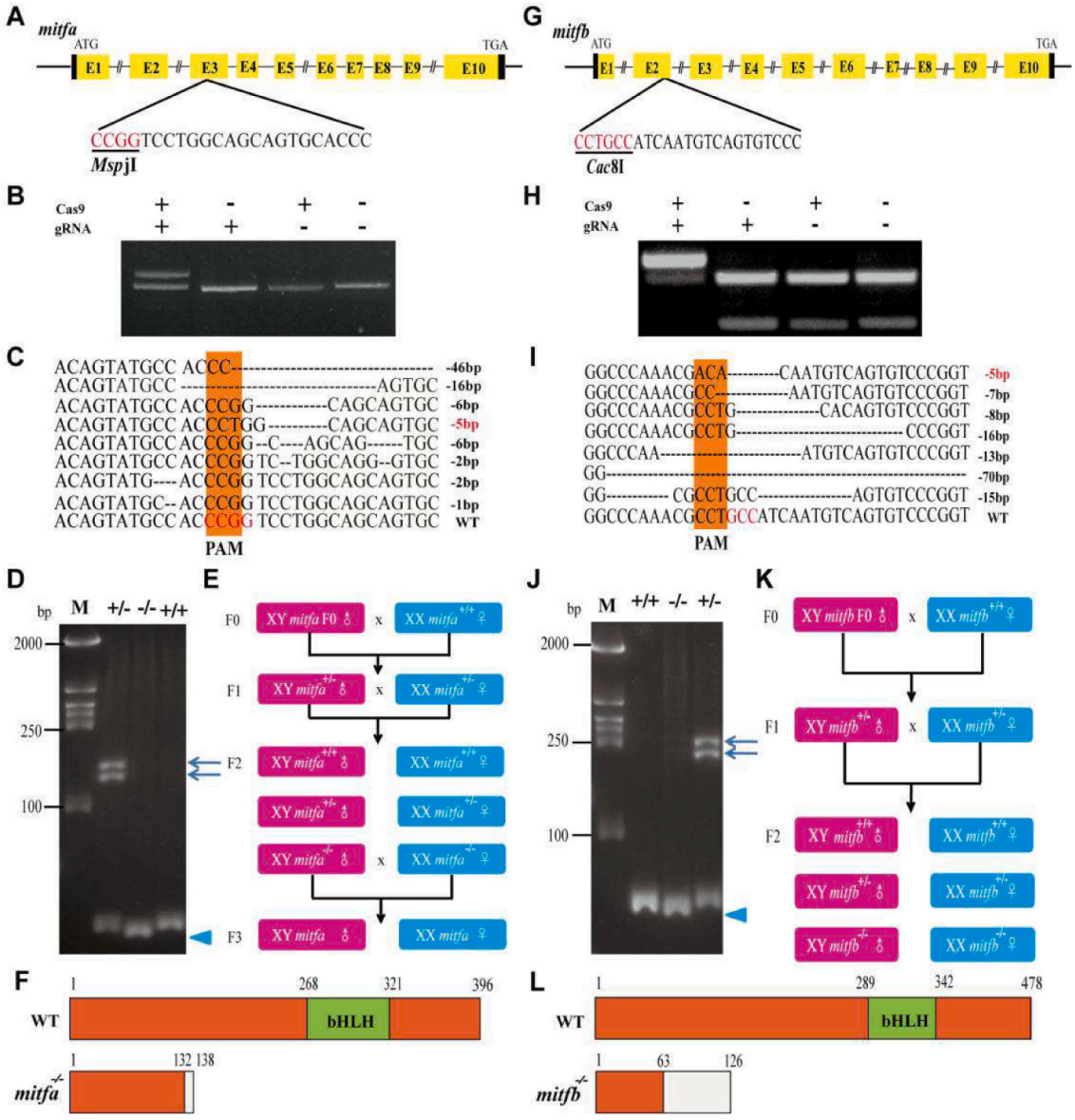

Fig. 1. Establishment of *mitfa*$^{-/-}$ (A-F) and *mitfb*$^{-/-}$ (G-L) mutant lines.
A, G: Gene structure of *mitfa* and *mitfb* showing the target site and the *Msp*jI and *Cac*8I restriction site, respectively. B, H: Restriction enzyme digestion of the amplified fragment of *mitfa* and *mitfb* using primers spanning the target site, respectively. The Cas9 mRNA and gRNA were added as indicated. C, I: Sanger sequencing results from the uncleaved band. The PAM is marked in orange. Deletions are marked by dashes (−) and numbers to the right of the sequences indicate the loss of bases for each allele. WT, wild type. D, J: Identification of *mitfa* and *mitfb* F2 genotypes by heteroduplex motility assay. Arrowheads show homoduplexes and arrows show heteroduplexes. E, K: Schematic diagram showing the breeding plans of *mitfa* and *mitfb* F0 to F2 fish. F, L: Protein structures of *mitfa* and *mitfb* showing the functional domains (orange) including bHLH DNA binding domain (green). Homozygous mutation of *mitfa* and *mitfb* led to truncated proteins of only 138 and 126 amino acids, respectively. (For interpretation of the references to color in this figure legend, the reader is referred to the web version of this article).

2.4. Pigment cell analysis of the trunk scales and caudal fins

Caudal fin and caudal peduncle of 150 dpf were photographed with a Nikon D7000 digital camera (Nikon, Japan) against a white background. The caudal fins of 150 and 180 dpf were removed with medical scissors, soaked in 0.65% Ringers' solution and directly observed with Olympus SZX16 stereomicroscope (Olympus, Japan) without cover slip under transparent or bright field. Scales at the bottom of the third dorsal fin rays (corresponding to the second trunk vertical bar) were separated directly with forceps. Scales were soaked in 0.65% Ringers' solution under cover slip, and were observed under Leica EM UC7 microscope (Leica, Germany). Image recording of pigment cells were conducted as quickly as possible after putting them in the Ringers' solution as the preparations are not stable. ACDSee Official Edition software and Adobe Illustrator CS6 were used to format the pictures. To analyze the number of melanophores and xanthophores, nine fish per group were anesthetized with tricaine methasulfonate (MS-222, Sigma-Aldrich, USA) and immersed in 10 mg/ml epinephrine (Sigma, USA) solution for 15 min to contract melanosomes and erythrosomes. The Image J software (Schneider et al., 2012) was used for relative iridophore content and pigment cell size analysis. GraphPad Prism 5.01 software (Graphpad, USA) was used to analyze and export the differences in the number and sizes of melanophores and xanthophores in *mitfa*$^{-/-}$, *mitfb*$^{-/-}$ and *mitfa*$^{-/-}$;*mitfb*$^{-/-}$ mutants and wild-type fish. Data values between each of the three different *mitf* genes' mutants and wild-type fish were statistically evaluated by one-way ANOVA with Duncan's post-hoc test. $P < 0.05$ was considered to be statistically significant, as indicated by different letters above the error bar. Data values between the 180 dpf

wild-type fish and *mitfa*$^{-/-}$;*mitfb*$^{-/-}$ mutants were tested by two-tailed Student's *t*-test (***, $P < 0.001$; **, $P < 0.01$; *, $P < 0.05$; ns, not significant) and expressed as mean ± SD.

2.5. Melanin quantification and melanin biosynthesis ability comparison

To analyze the melanin content, three fish per group were anesthetized with tricaine methasulfonate (MS-222, Sigma-Aldrich, USA). Skin sample suspensions were solubilized in 8 M urea/1 M sodium hydroxide and cleared by centrifugation at 10,700*g* for 10 min. Chloroform was added to the supernatants to remove fatty impurities. Skin samples were cleared by centrifugation at 10,700*g* for 10 min and analyzed for absorbance at 400 nm, as we shown in our previous studies (Wang et al., 2022b).

2.6. Comparative analysis on the pigmentary basis of wild-type, *mitfa*$^{-/-}$;*mitfb*$^{-/-}$ mutants, *pmela*$^{-/-}$;*pmelb*$^{-/-}$ mutants and *hps4*$^{-/-}$ mutants

The dorsal scales and caudal fins of wild-type, *mitfa*$^{-/-}$;*mitfb*$^{-/-}$ mutants, *pmela*$^{-/-}$;*pmelb*$^{-/-}$ mutants and *hps4*$^{-/-}$ mutants at 180 dpf were prepared and analyzed with the same methods showed in "Pigment cell analysis of the trunk scales and caudal fins" section above. GraphPad Prism 5.01 software (Graphpad, USA) was used to analyze and export the differences in the numbers of pigmented melanophores, xanthophores, erythrophores, relative iridophore content and melanin content in *mitfa*$^{-/-}$;*mitfb*$^{-/-}$ mutants, *pmela*$^{-/-}$;*pmelb*$^{-/-}$ mutants, *hps4*$^{-/-}$ mutants and wild-type fish. Data values between each of the three different color mutants and wild-type fish were statistically evaluated by one-way ANOVA with Duncan's post-hoc test. $P < 0.05$ was considered to be statistically significant, as indicated by different letters above the error bar.

2.7. Modeling and image processing

Sharp 3D software (Sharp 3D systems, Hungary), ACDSee Official Edition software (ACDSystems, Canada), Adobe Illustrator CS6 (Adobe Inc. USA) and Image J software (Schneider et al., 2012) were used to format the pictures and modeling of the phenotypes, pigment cell development and pigment cell relative abundance of the wild-type fish and the color mutants.

3. Results

3.1. Establishment of the three mutant strains

The F0 founders were screened by restriction enzyme digestion and Sanger sequencing (Fig. 1B, C, H and I). The *mitfa* and *mitfb* mutant fish with a high mutation rate (over 75%) were raised to sexual maturity and mated with wild-type tilapia to create the F1 fish. In *mitfa* F0 chimera, small white patches deficient in melanophores were detected on the trunk and fins, while no significant differences in body color were detected in *mitfb* F0 chimeras.

The F1 mutant fish were obtained by crossing an F0 XY male with a wild-type XX female. Heterozygous *mitfa* F1 offspring with a − 5 bp deletion in the third exon were selected to breed the F2 generation (Fig. 1C-E). Heterozygous *mitfb* F1 offspring with a − 5 bp deletion in the second exon were also selected to breed the F2 generation (Fig. 1I-K). *mitfa;mitfb* F1 generation were produced by firstly mating male F0 *mitfb*-positive fish with a *mitfa* − 5 bp F2 homozygous mutant, then heterozygous *mitfa;mitfb* F1 offspring with a − 5 bp deletion in *mitfa* and − 5 bp deletion in *mitfb* were selected to breed the F2 generation (Fig. S1). A heteroduplex mobility assay identified the heterozygous *mitfa*$^{+/-}$ and *mitfb*$^{+/-}$ individuals as those possessing both heteroduplex and homoduplex amplicons vs. the *mitfa*$^{+/+}$ and *mitfa*$^{-/-}$, *mitfb*$^{+/+}$ and *mitfb*$^{-/-}$ individuals with only homo-duplex amplicons (Fig. 1D and J). Homozygous mutation of *mitfa* and *mitfb* led to truncated proteins of only 138 and 126 amino acids, respectively (Fig. 1F and L).

3.2. Hypo-pigmentation was detected in mitf mutants at 4, 5 and 7 dpf

We characterized the phenotype of the mutant fish in their early developmental stages. In wild-type fish, many melanophores were detected on the yolk sac, densely distributed along the vascular network. Slight black pigmentation was detected on the iris and RPE at 4 dpf (Fig. 2A). At 5 dpf, increasing numbers of melanophores were detected on the head and peritoneum, melanophores had migrated from the yolk sac to the operculum and peritoneum, and there was a significant increase of iridophores in the peritoneum and iris (Fig. 2B and B'). Similar patterns were detected in the 7 dpf fish, and increasing numbers of melanophores were also detected in the trunk (Fig. 2C and C').

In *mitfa*$^{-/-}$ mutants, a few hypo-pigmented melanophores were detected on the yolk sac, and the iris and RPE were slightly pigmented at 4 dpf (Fig. 2D). A few melanophores were detected on the yolk sac, and they migrated towards the operculum and peritoneum. At 5 dpf many iridophores were detected in the peritoneum and iris, and the peritoneum was partially transparent as fewer melanophores appeared compared with the wild-type fish (Fig. 2E and E'). Some hypo-pigmented melanophores and many large-sized xanthophores were detected on top of the head, and the yolk sac had a few tiny melanophores. The peritoneum was still partially transparent at 7 dpf (Fig. 2F and F').

In *mitfb*$^{-/-}$ mutants, many melanophores were detected on the yolk sac, and the iris and RPE were also slightly pigmented at 4 dpf (Fig. 2G). At 5 dpf some hypo-pigmented melanophores were detected on the yolk sac, and the iris and RPE were pigmented with many iridophores and melanin, respectively (Fig. 2H and H'). At 7 dpf many melanophores were detected on top of the head, on the trunk and the peritoneum. Migration of melanophores was also detected from the yolk sac to the operculum and peritoneum at this time (Fig. 2I and I').

In *mitfa*$^{-/-}$;*mitfb*$^{-/-}$ mutants, a few tiny hypo-pigmented melanophores were detected on the yolk sac. At 4 dpf the iris and RPE were slightly pigmented, similar to the wild-type fish and the single mutants (Fig. 2J) and a few tiny hypo-pigmented melanophores were detected on the yolk sac. The iris and RPE were pigmented with many iridophores and melanin, respectively. At 5 dpf some melanophores were detected in the partially transparent peritoneum (Fig. 2K and K'). Some melanophores were detected on the top head and many iridophores in the peritoneum. At 7 dpf the peritoneum was still partially transparent due to the significant reduction of melanophores compared to wild-type fish (Fig. 2L and L').

From the dorsal view, some tiny hypo-pigmented melanophores were observed on top of the head, while some normal melanophores were detected in the peritoneum of *mitfa*$^{-/-}$ mutants at 7 dpf (Fig. 2M). In contrast, at 7 dpf the *mitfa*$^{-/-}$;*mitfb*$^{-/-}$ mutants had a few tiny hypo-pigmented melanophores on top of the head, and a more transparent peritoneum was observed, due to additional melanophore loss compared to the *mitfa*$^{-/-}$ mutants (Fig. 2N). Importantly, the RPE in both *mitfa*$^{-/-}$ single and *mitfa*$^{-/-}$;*mitfb*$^{-/-}$ double mutants was black without any hypo-pigmentation.

3.3. Hypo-pigmentation in mitf mutants and yellowish body color in *mitfa*$^{-/-}$;*mitfb*$^{-/-}$ mutants were detected at 12, 60 and 90 dpf

We also characterized the phenotypes of the mutants before and after metamorphosis during bar formation. In wild-type fish, no bars were detected, and melanophores were spread evenly across the whole trunk at 12 dpf (Fig. 3A). Black bars separated by light colored inter-bars were detected at 60 dpf. A higher density of melanophores were detected in the bar regions at this time point. They may have simply appeared at this location by cell division from existing melanophores, or by differentiation of stem cells in this region. Iridophores sharply increased in the caudal peduncle (Fig. 3B and B'). Strong black bars separated by

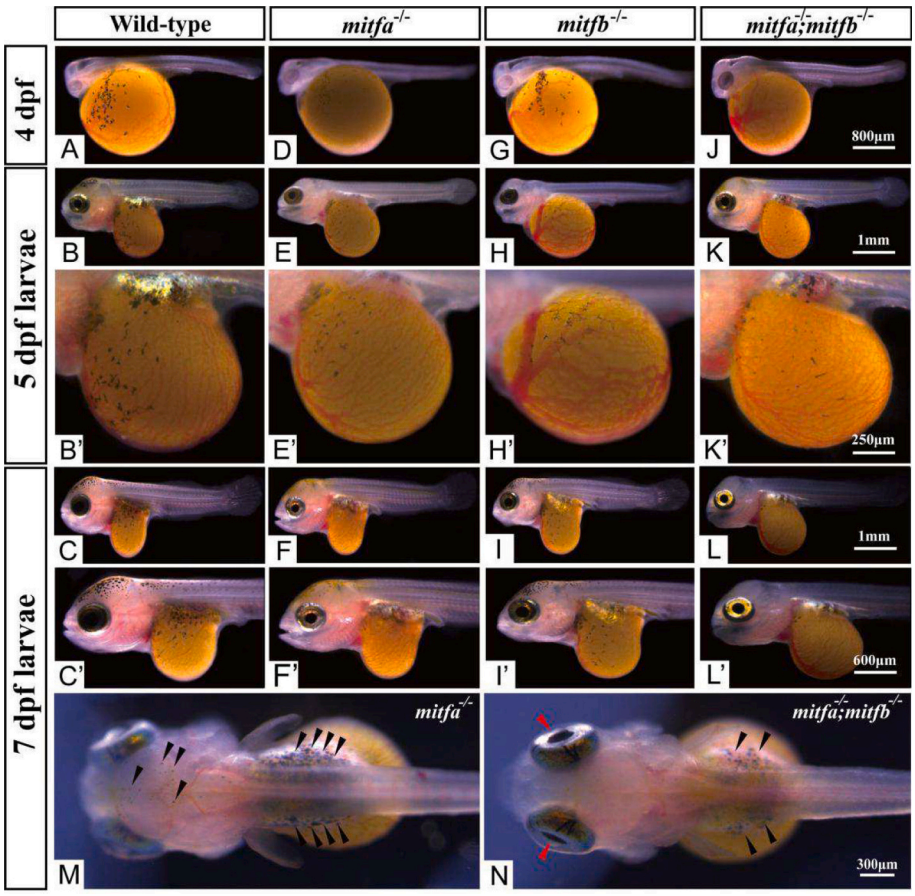

Fig. 2. Melanophores were significantly decreased in *mitfa*$^{-/-}$, *mitfb*$^{-/-}$ and *mitfa*$^{-/-}$; *mitfb*$^{-/-}$ mutants at 4 (A, D, G and J), 5 (B, E, H, K, B′, E', H′ and K′) and 7 dpf (C, F, I, L, C′, F′, I′, L', M and N).
A: Wild-type fish with many melanophores on the yolk sack and pigmented RPE. B and B′: Wild-type fish with many melanophores on the yolk sack, heavily pigmented RPE, iridophore enriched peritoneum and iris. C and C′: Wild-type fish with increased melanophores on the yolk sack, peritoneum, top head and trunk, and heavily pigmented RPE. D: *mitfa*$^{-/-}$ mutants with a few melanophores on the yolk sack and unaffected RPE. E and E': *mitfa*$^{-/-}$ mutants with a few melanophores on the yolk sack, black RPE, iridophore enriched peritoneum and iris. F and F′: *mitfa*$^{-/-}$ mutants with some melanophores on the yolk sack, peritoneum and top head, and black RPE. The peritoneum was partially transparent and the top head was yellowish due to the reduction of melanophores. G: *mitfb*$^{-/-}$ mutants with less melanophores on the yolk sack than in wild-type fish but higher than in *mitfa*$^{-/-}$ mutants and unaffected RPE. H and H′: *mitfb*$^{-/-}$ mutants with a few melanophores on the yolk sack, head and trunk, black RPE, and iridophores enriched peritoneum and iris. I and I′: *mitfb*$^{-/-}$ mutants with many melanophores on the yolk sack, peritoneum and top head, and black RPE. J: *mitfa*$^{-/-}$; *mitfb*$^{-/-}$ mutants with few melanophores on the yolk sack and pigmented RPE. K and K′: *mitfa*$^{-/-}$;*mitfb*$^{-/-}$ mutants with a few tiny melanophores on the yolk sack and head, unaffected RPE, and iridophore enriched peritoneum and iris. L and L': *mitfa*$^{-/-}$; *mitfb*$^{-/-}$ mutants with a few melanophores on the yolk sack and top head, unaffected RPE, and more transparent peritoneum than *mitfa*$^{-/-}$ mutants. M: *mitfa*$^{-/-}$ mutants with tiny melanophores on the top head and normal sized melanophores on the peritoneum. N: *mitfa*$^{-/-}$;*mitfb*$^{-/-}$ mutants with unaffected RPE (red arrow heads), fewer melanophores (black arrow heads) on top head and peritoneum than *mitfa*$^{-/-}$ mutants. (For interpretation of the references to color in this figure legend, the reader is referred to the web version of this article).

iridescent inter-bars were detected in wild-type fish at 90 dpf, which made them look much like the adult fish (Fig. 3C).

In *mitfa*$^{-/-}$ mutants, melanophores were heavily reduced on the trunk surface at 12 dpf (Fig. 3D). Hypo-pigmentation with weak bars separated by iridescent inter-bars was observed in the mutants at 60 dpf (Fig. 3E and E'). Weak gray vertical bars separated by yellow inter-bars were detected in mutants at 90 dpf, and the trunk surface below the lateral line showed a more iridescent color. Melanophores were reduced and iridophores increased in numbers (Fig. 3F).

In *mitfb*$^{-/-}$ mutants, no apparent changes were observed in number or morphology of melanophores or other pigment cell types at 12 dpf (Fig. 3G). At 60 dpf, the *mitfb*$^{-/-}$ mutants displayed a phenotype similar to the wild-type fish, with the trunk slightly hypo-pigmented. Both bars and inter-bars were filled with melanophores (Fig. 3H and H'). At 90 dpf, the trunk was slightly hypo-pigmented and bars were occasionally detected. A few loose round black spots were detected along the lateral line (Fig. 3I). Additionally, a few of the mutants displayed iridescent microphthalmia eyes which may affect visual recognition and increase stress in the mutants. Mutant fish with one iridescent microphthalmia eye displayed almost the same body color as those mutants with normal eyes (Fig. S2).

In *mitfa*$^{-/-}$;*mitfb*$^{-/-}$ mutants, more serious loss of melanophores in the trunk surface than *mitfa*$^{-/-}$ mutants was detected at 12 dpf. Xanthophore numbers rose sharply on the head and the fish displayed yellowish body color (Fig. 3J). The double mutants displayed even more serious hypo-pigmentation with no bars compared with the *mitfa*$^{-/-}$ or *mitfb*$^{-/-}$ mutants at 60 dpf. Some randomly-distributed black spots composed of macro-melanophores were detected in the trunk of the double mutants, but the pigmentation of the RPE was normal (Fig. 3K and K'). At 90 dpf, significant hypo-pigmentation was detected in the double mutants. No bars were detected in the trunk. Most of the fish displayed randomly distributed large spots of macro-melanophores and small spots composed of ordinary melanophores (Fig. 3L). Additionally, a few of the double mutants displayed iridescent microphthalmia eyes, as observed in *mitfb*$^{-/-}$ mutants. The double mutants with two iridescent microphthalmia eyes also displayed very serious hypo-pigmentation, but in a milder way than those mutants with normal eye size (Fig. S2).

It should be mentioned that macro-melanophores, first appearing on top of the head at 5 dpf of wild-type fish, were also detected at 12 dpf, and were still detectable in the head and trunk (mostly distributed in the hyper-pigmented vertical bars) at 30 dpf (Fig. S3). At 60 and 90 dpf, these macro-melanophores were detected in the randomly distributed black spots observed in the head and trunk in *mitfa*$^{-/-}$;*mitfb*$^{-/-}$ mutants. Additionally, the *mitfa*$^{-/-}$;*mitfb*$^{-/-}$ mutants were detected with slight yellow body color at 60 and 90 dpf, while an obvious accumulation of reddish and yellow coloration in trunk and fins at 4 months (120 dpf) (Fig. S4).

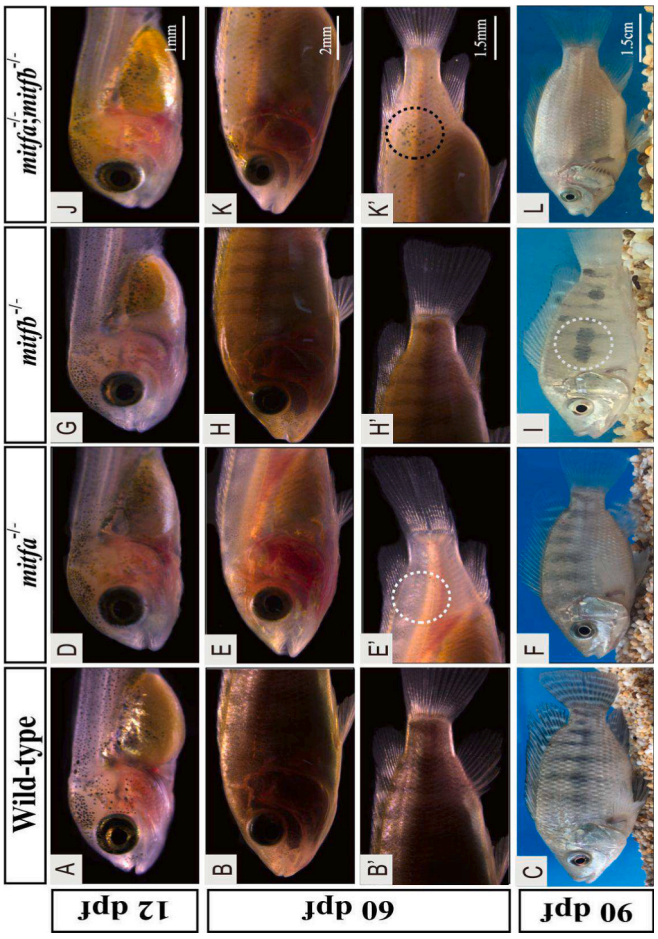

Fig. 3. Melanophores were significantly decreased, and the xanthophores and iridophores were also influenced in *mitfa*$^{-/-}$, *mitfb*$^{-/-}$ and *mitfa*$^{-/-}$;*mitfb*$^{-/-}$ mutants at 12 (A, D, G and J), 60 (B, E, H, K, B′, E', H′ and K′) and 90 dpf (C, F, I and L).

A: Wild-type fish with no pigmented vertical bars in the trunk. B and B′: Wild-type fish with heavily pigmented vertical bars in the trunk. C: Wild-type fish with obvious vertical bars. D: *mitfa*$^{-/-}$ mutants with reduced melanophores. E and E': *mitfa*$^{-/-}$ mutants with hyper-pigmentation but with weak vertical bars and more white iridophores (white dotted circle) in trunk. F: *mitfa*$^{-/-}$ mutants with hypo-pigmentation but with weak vertical bars in the trunk and fins. G: *mitfb*$^{-/-}$ mutants with less melanophores than the wild-type fish. H and H′: *mitfb*$^{-/-}$ mutants with slight hyper-pigmentation in trunk and fins and with color pattern similar to the wild-type fish. I: *mitfb*$^{-/-}$ mutants with loose black round spots in trunk. J: *mitfa*$^{-/-}$;*mitfb*$^{-/-}$ mutants with more serious hypo-pigmentation than *mitfa*$^{-/-}$ mutants. K and K′: *mitfa*$^{-/-}$;*mitfb*$^{-/-}$ mutants with white body color in the trunk and fins and with randomly spread macro-melanophore-composed black spots (black dotted circle) in the trunk. L: *mitfa*$^{-/-}$; *mitfb*$^{-/-}$ mutants with white body color and with randomly spread macro-melanophores in the trunk and fins.

3.4. Changes in melanophore and xanthophore number and size in dorsal scales at 150 dpf

Body scales from the top of the second vertical bar were used to analyze the pigment cells in trunk (Fig. 4A-D). Under transparent field, the scales were filled with mature melanophores and small and shrunken xanthophores in wild-type fish (Fig. 4E and E').

In *mitfa*$^{-/-}$ mutants, melanophores were obviously reduced compared with the wild-type fish, and most of them were in a state of fragmentation or apoptosis. Xanthophores were reduced in the mutants, but obviously larger than those of the wild-type fish (Fig. 4F and F').

In *mitfb*$^{-/-}$ mutants, the number of melanophores was reduced compared with the wild-type fish. Many melanophores were shrunken, which was consistent with the light-colored trunk with occasionally visible black vertical bars. The xanthophores were reduced in number, but increased in size compared with the wild-type fish (Fig. 4G and G').

The *mitfa*$^{-/-}$;*mitfb*$^{-/-}$ mutants showed even fewer hypo-pigmented melanophores, than *mitfa*$^{-/-}$ mutants. The iridophores were abundant, but displayed white color only, not the iridescent colors of the wild-type fish (Fig. 4H and H'). The sizes of xanthophores were larger than in wild-type fish.

Quantification of pigment cell numbers showed that pigmented melanophores were significantly reduced in *mitfb*$^{-/-}$ mutants, more reduced in *mitfa*$^{-/-}$ mutants and most reduced in *mitfa*$^{-/-}$;*mitfb*$^{-/-}$ mutants (Fig. 4I). Interestingly, the xanthophores were also significantly reduced and similar in number in *mitfa*$^{-/-}$, *mitfb*$^{-/-}$ and *mitfa*$^{-/-}$;*mitfb*$^{-/-}$ mutants (Fig. 4J). The size of the xanthophores was significantly larger in the three mutants compared with that of the wild-type fish (Fig. 4K).

3.5. Melanophores were significantly decreased, and iridophores were significantly increased in caudal fins and caudal peduncle in mitf mutants at 150 dpf

The central part of the caudal fin from fish at 150 dpf was used for pigment cell analysis. The wild-type fish showed heavily pigmented vertical bars and light-colored inter-bars in the caudal fin and caudal peduncle (Fig. 5A). The caudal fins were filled with mature melanophores and xanthophores. Some of them were even attached on the fin rays (Fig. 5B and B').

In the *mitfa*$^{-/-}$ mutants, some melanophores were detected in the caudal fin and caudal peduncle, with weak gray banding (Fig. 5C). The melanophores were obviously reduced compared with the wild-type fish. Additionally, the melanophores only spread between the fin rays. In contrast, increased iridophores were observed, especially in the regions typically occupied by melanophores in the wild-type fish (Fig. 5D and D').

In the *mitfb*$^{-/-}$ mutants, the caudal fin was slight hypo-pigmented, both bars and inter-bars were observed with mostly black pigmentation in the caudal fin and caudal peduncle (Fig. 5E). Fewer melanophores, but many xanthophores and erythrophores, were detected in the caudal fin in the *mitfb*$^{-/-}$ mutants. Many of the melanophores were in a contracted state (Fig. 5F and F').

In the *mitfa*$^{-/-}$;*mitfb*$^{-/-}$ mutants, the caudal fin and caudal peduncle were yellow. However, a few loose weak black spots were still detected (Fig. 5G). Fewer melanophores were detected in the caudal fin and caudal peduncle than in *mitfa*$^{-/-}$ mutants. In contrast, the caudal fin, including the fin rays, were filled with white iridophores (Fig. 5H and H').

Quantification of the pigment cells showed that the pigmented melanophores were significantly reduced in *mitfb*$^{-/-}$ mutants, more reduced in *mitfa*$^{-/-}$ mutants, and most reduced in *mitfa*$^{-/-}$;*mitfb*$^{-/-}$ mutants (Fig. 5I). The numbers of xanthophores remained unchanged in *mitfa*$^{-/-}$, *mitfb*$^{-/-}$ and *mitfa*$^{-/-}$;*mitfb*$^{-/-}$ mutants compared with the wild-type fish (Fig. 5J). The iridophores were significantly increased in *mitfa*$^{-/-}$, *mitfb*$^{-/-}$ and *mitfa*$^{-/-}$;*mitfb*$^{-/-}$ mutants compared with the wild-type fish (Fig. 5K).

3.6. Melanophores were significantly decreased, while erythrophores and xanthophores were significantly increased in dorsal scales and caudal fin of *mitfa*$^{-/-}$;*mitfb*$^{-/-}$ mutants at 180 dpf

At 180 dpf, wild-type fish had 7 hyper-pigmented bars and 8 light-pigmented inter-bars (Fig. 6A). The RPE was black, and the iris was filled with melanophores (Fig. 6B). The dorsal scales had many melanophores with branching-like clusters, surrounded by iridescent purple or orange iridophores. Additionally, many neighboring small xanthophores with folded shapes were detected (Fig. 6C). The caudal fin was detected with many melanophores and some xanthophores, iridophores

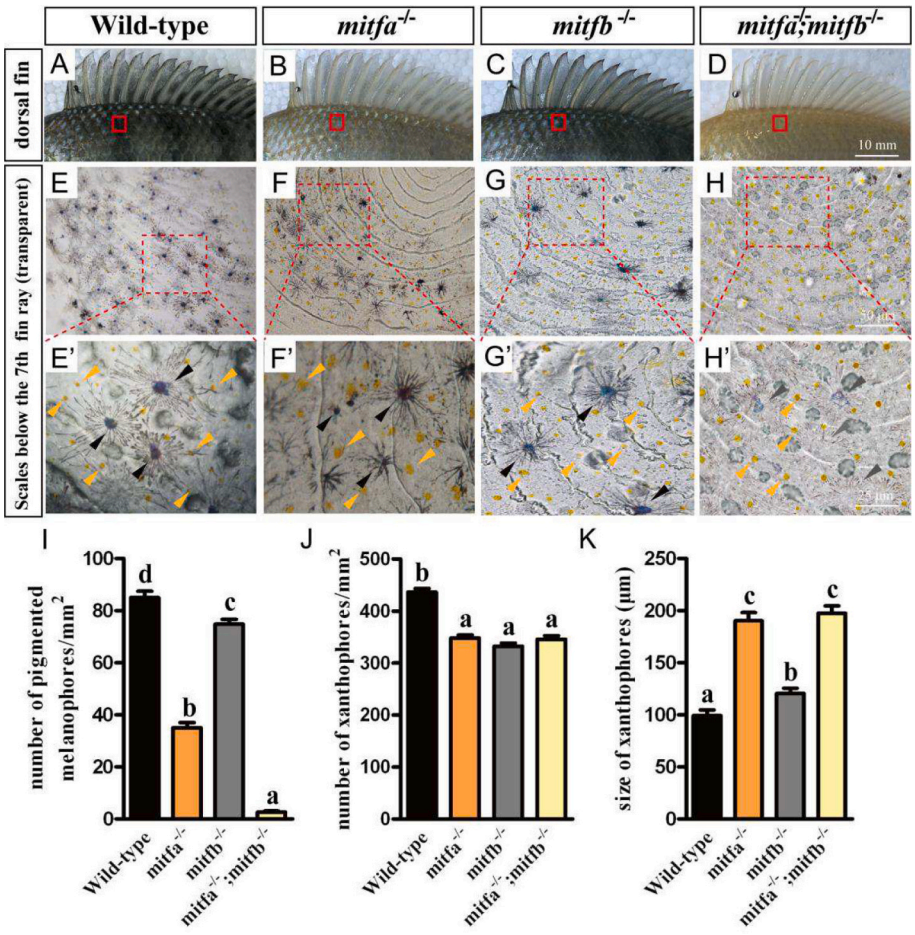

Fig. 4. Melanophores and xanthophores were significantly decreased, but xanthophores were significantly increased in sizes in dorsal trunk, dorsal fin (A-D) and scales (*E*-H and higher magnification E'-H′) in *mitfa*$^{-/-}$, *mitfb*$^{-/-}$ and *mitfa*$^{-/-}$;*mitfb*$^{-/-}$ mutants at 150 dpf.

A: Wild-type fish displayed black body color with plenty of melanophores. B: The *mitfa*$^{-/-}$ mutants displayed yellowish body color with less melanophore than *mitfb*$^{-/-}$ mutants. C: The *mitfb*$^{-/-}$ mutants with less melanophores than wild-type fish. D: *mitfa*$^{-/-}$;*mitfb*$^{-/-}$ mutants with hypo-pigmentation and no bars. E and E': Scales (red square) from wild-type fish with many mature stretched melanophores (black arrow heads) surrounded by purple and blue colored iridophores and round xanthophores (yellow arrow heads). F and F′: Scales (red square) from *mitfa*$^{-/-}$ mutants with significantly reduced and apoptotic melanophores (black arrow heads) surrounded by larger sized xanthophores (yellow arrow heads) and purple colored iridophores. G and G': Scales (red square) from *mitfb*$^{-/-}$ mutants with significantly reduced melanophores (black arrow heads) surrounded by blue colored iridophores. H and H′: Scales (red square) from *mitfa*$^{-/-}$;*mitfb*$^{-/-}$ mutants with a few hypo-pigmented melanophores (gray arrow heads) and many xanthophores (yellow arrow heads) and iridophores. I and J: Quantification on the numbers of melanophores and xanthophores in dorsal scales. K: Quantification on the sizes of xanthophores in dorsal scales. Data are expressed as the mean ± SD in I—K (n = 9). Significant differences in the data among groups were tested by one-way ANOVA with Duncan's post-hoc test. $P < 0.05$ was considered to be statistically significant, indicated by different letters above the error bar. (For interpretation of the references to color in this figure legend, the reader is referred to the web version of this article).

and erythrophores (Fig. 6D and D').

What was striking was that with development, the *mitfa*$^{-/-}$;*mitfb*$^{-/-}$ mutants showed vastly increasing amounts of red and yellow body color, especially in the sexually maturated mutants. The mutants no longer showed obvious bars or inter-bars (Fig. 6E). The RPE was still black, and the iris was filled with many iridophores and increasing reddish carotenoids pigmentation (Fig. 6F). The dorsal scales had hypo-pigmented melanophores with branching-like clusters, surrounded by many hypertrophic xanthophores. Increasing numbers of erythrophores were also detected (Fig. 6G). The caudal fin had no pigmented melanophores but still contained a large number of erythrophores and xanthophores (Fig. 6H and H').

Quantification of the pigment cells showed that the pigmented melanophores were significantly reduced or even absent in dorsal scales and caudal fin of *mitfa*$^{-/-}$;*mitfb*$^{-/-}$ mutants (Fig. 6I and K). In contrast, the total number of erythrophores and xanthophores (which were hard to be distinguished in caudal fins) were significantly increased in the mutants (Fig. 6J and L). Melanin content in dorsal skin of the mutants was also significantly lower than that in wild-type fish (Fig. 6M).

3.7. Disruption of the genes mitf, pmel and hps4 that function in different aspects of melanogenesis led to different body colors with different relative abundance of pigment cells

Recently, we have successfully mutated both *pmel* duplicates and *hps4* in tilapia (Wang et al., 2022a, 2022b). The *mitfa*$^{-/-}$;*mitfb*$^{-/-}$, *pmela*$^{-/-}$;*pmelb*$^{-/-}$ and *hps4*$^{-/-}$ mutants displayed different body colors with different relative abundance of pigment cells (Fig. 7, Fig. S5). The wild-type fish displayed black vertical bars and light colored inter-bars, and the whole fish was black in coloration (Fig. 7A) The dorsal scales had many mature melanophores surrounded by small round xanthophores (Fig. 7B). The *mitfa*$^{-/-}$;*mitfb*$^{-/-}$ mutants displayed red and yellow color in trunk and fins (Fig. 7C) with increased numbers of erythrophores, and fewer hypo-pigmented melanophores in clusters. The dorsal scales had fewer but larger sized xanthophores (Fig. 7D). The *pmela*$^{-/-}$;*pmelb*$^{-/-}$ mutants displayed a golden body color (Fig. 7E), and the dorsal scales had unclusterd small round melanophores, and more and larger sized xanthophores (Fig. 7F). The *hps4*$^{-/-}$ mutants showed a silver-white body color, with slight reddish pigmentation in trunk, fins and iris (Fig. 7G), with no pigmented melanophores, but with more and larger sized xanthophores in the dorsal scales (Fig. 7H).

Quantification of the pigment cells in dorsal scales revealed that the wild-type fish has the highest number of pigmented melanophores. The *pmela*$^{-/-}$;*pmelb*$^{-/-}$ mutants had significantly fewer melanophores than the wild-type fish, but still significantly more than the *mitfa*$^{-/-}$;*mitfb*$^{-/-}$ and *hps4*$^{-/-}$ mutants (Fig. 7I). The xanthophore numbers in dorsal scales of the *pmela*$^{-/-}$;*pmelb*$^{-/-}$ and *hps4*$^{-/-}$ mutants were the highest and displayed no significant differences between them, but were significantly higher than those in the wild-type fish which in turn were significant higher than the *mitfa*$^{-/-}$;*mitfb*$^{-/-}$ mutants (Fig. 7J). The number of erythrophores in the *mitfa*$^{-/-}$;*mitfb*$^{-/-}$ mutants was significantly higher than that of the *pmela*$^{-/-}$;*pmelb*$^{-/-}$ mutants which were significantly higher than that of the *hps4*$^{-/-}$ mutants and wild-type fish, indicating an earlier accumulation of erythrophores and carotenoids in the *mitfa*$^{-/-}$;*mitfb*$^{-/-}$ mutants (Fig. 7K). The melanin content in the *mitfa*$^{-/-}$;*mitfb*$^{-/-}$ and *pmela*$^{-/-}$;*pmelb*$^{-/-}$ mutants were significantly lower than that in the wild-type fish, but significantly higher than that in the *hps4*$^{-/-}$ mutants, (Fig. 7L).

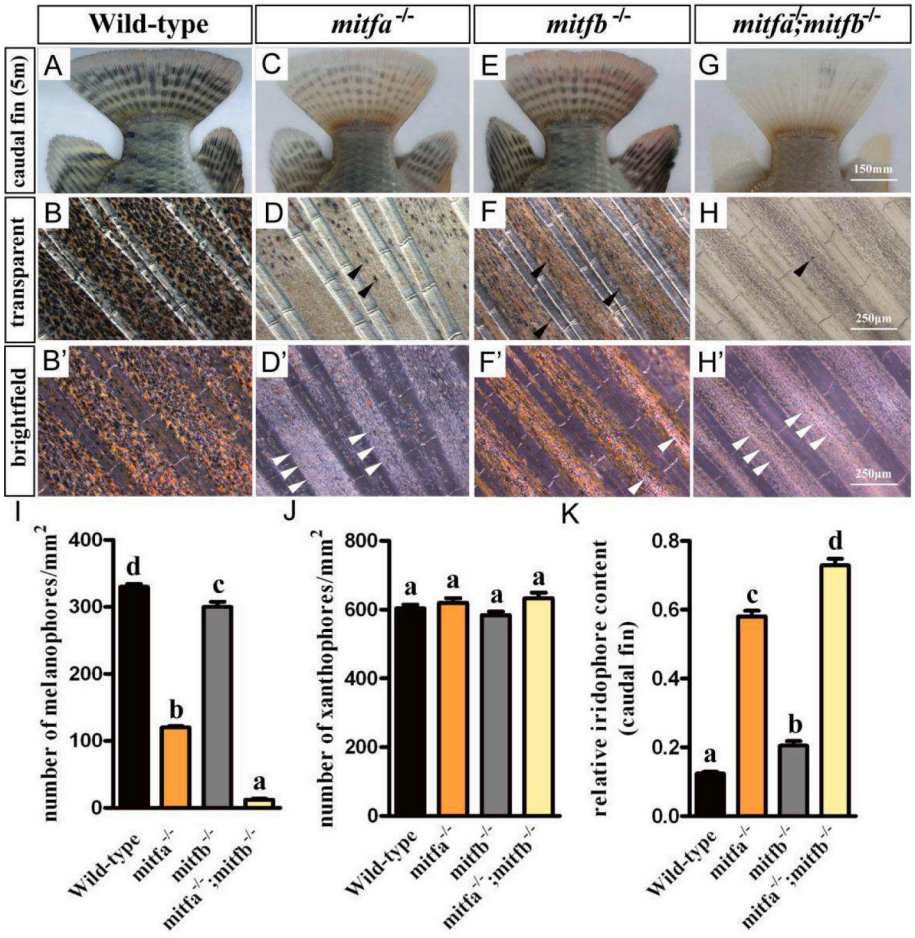

Fig. 5. Melanophores were significantly decreased, xanthophores unchanged but iridophores significantly increased in caudal fins and caudal peduncle in *mitfa*$^{-/-}$, *mitfb*$^{-/-}$ and *mitfa*$^{-/-}$;*mitfb*$^{-/-}$ mutants at 150 dpf.

A: Wild-type fish with bars and light colored interbars. B and B′: Wild-type fish with many mature melanophores (some of them attached on the fin rays) and xanthophores. C: *mitfa*$^{-/-}$ mutants with hypo-pigmentation, but still with gray weak bars. D and D′: *mitfa*$^{-/-}$ mutants with significant less melanophores (black arrow heads) than wild-type fish and iridophores (white arrow heads) occupied the original melanophores' territory. E: *mitfb*$^{-/-}$ mutants with slight hypo-pigmentation, but still with heavily pigmented bars. F and F′: *mitfb*$^{-/-}$ mutants with significantly reduced melanophores (black arrow heads, most of them in melanosome-aggregated state) and unchanged xanthophores and erythrophores compared with wild-type fish. G: *mitfa*$^{-/-}$;*mitfb*$^{-/-}$ mutants with serious hypo-pigmentation and yellow-white caudal fin. H and H′: *mitfa*$^{-/-}$;*mitfb*$^{-/-}$ mutants with a few melanophores (black arrow heads) and many white iridophores (white arrow heads) in the caudal fin. I-K: Quantificaiton on the numbers of melanophores, xanthophores and relative iridophore content in caudal fin. Data are expressed as the mean ± SD (n = 9). Significant differences in the data among groups were tested by one-way ANOVA with Duncan's post-hoc test. $P < 0.05$ was considered to be statistically significant, indicated by different letters above the error bar. (For interpretation of the references to color in this figure legend, the reader is referred to the web version of this article).

Additionally, the relative pigment cell abundance in caudal fins of the *mitfa*$^{-/-}$;*mitfb*$^{-/-}$ mutants, *pmela*$^{-/-}$;*pmelb*$^{-/-}$ mutants and *hps4*$^{-/-}$ mutants were similar to the results we showed in dorsal scales (Fig. S5).

4. Discussion

4.1. Mitf is fundamental for teleost body color formation

As the most important transcription factor for pigmentation disorders, the phenotypes of the mutants have received continuous attention for nearly a century. Studies on zebrafish and medaka have revealed some mechanisms for color patterning, which were of great significance for the studies of color pattern formation in teleosts (Lister et al., 1999; Sugimoto, 2002; Kelsh, 2004; Parichy, 2007; Singh and Nüsslein-Volhard, 2015). Research on other colorful teleost species, including cichlids, has lagged far behind compared with these model fish. Cichlids color patterns may be structured by unique mechanisms that do not have counterparts in model fish. The vast number of color patterns found among cichlid species can serve as a model system for the color patterns of teleosts more generally (Wang et al., 2021a). In this study, we focused on *mitf*, the most important gene controlling melanogenesis and melanoblast migration and specification (Hou and Pavan, 2008). As a fundamental transcription factor for melanoblast differentiation, melanogenesis and melanophore development, it has been well documented in color patterning and body color differentiation of humans (George et al., 2016), mice (Hodgkinson et al., 1993), dogs (Körberg et al., 2014), mink (*Neovison vison*) (Song et al., 2017), Peking ducks (Zhou et al., 2018), xenopus (Kawasaki et al., 2008), zebrafish (Lister et al., 1999; Taylor et al., 2011), koi carps (Liu et al., 2016), fighting fish (Wang et al., 2021b) and many other species. In human beings and mice, this gene is related to albinism, hearing loss and microphthalmia (George et al., 2016; Hodgkinson et al., 1993; Hou and Pavan, 2008). In mink and Peking ducks, this gene was found to be related to white hair and white plumage formation, and thus important for the economic value of the two species (Song et al., 2017; Zhou et al., 2018). Additionally, it has also been reported that *mitf* is closely related to the development and division of melanocytes in melanoma, a skin disease of human and zebrafish (Levy et al., 2006; Taylor et al., 2011). Therefore, it is of great significance for us to study this gene in tilapia as melanophores are the major pigment cells for tilapia body color formation.

Using CRISPR/Cas9 gene editing, we mutated both *mitfa* and *mitfb* in tilapia and successfully obtained the *mitfa*$^{-/-}$, *mitfb*$^{-/-}$ and *mitfa*$^{-/-}$;*mitfb*$^{-/-}$ mutants. Melanophores were significantly reduced in *mitfa*$^{-/-}$;*mitfb*$^{-/-}$ double mutants compared with the *mitfa*$^{-/-}$ and *mitfb*$^{-/-}$ single mutants and wild-type fish, which again confirmed the roles of *mitf* in melanophore differentiation, melanophore survival and melanogenesis. In the *mitfa*$^{-/-}$;*mitfb*$^{-/-}$ mutants, randomly distributed black spots composed of macro-melanophores were detected in the body in juvenile stages (obvious at 90 dpf, but disappeared at 120 dpf), which was similar to the phenotypes of mouse and dog *mitf* mutants (Hodgkinson et al., 1993; Körberg et al., 2014). These macro-melanophores were probably leftover early larval melanophores. They could be produced either from maternal transcripts, or by whatever regulatory pathway was turning on melanosomes in the RPE.

Strikingly, the *mitfa*$^{-/-}$;*mitfb*$^{-/-}$ mutants showed increasing amounts of reddish pigmentation at 120 dpf, suggesting proliferation

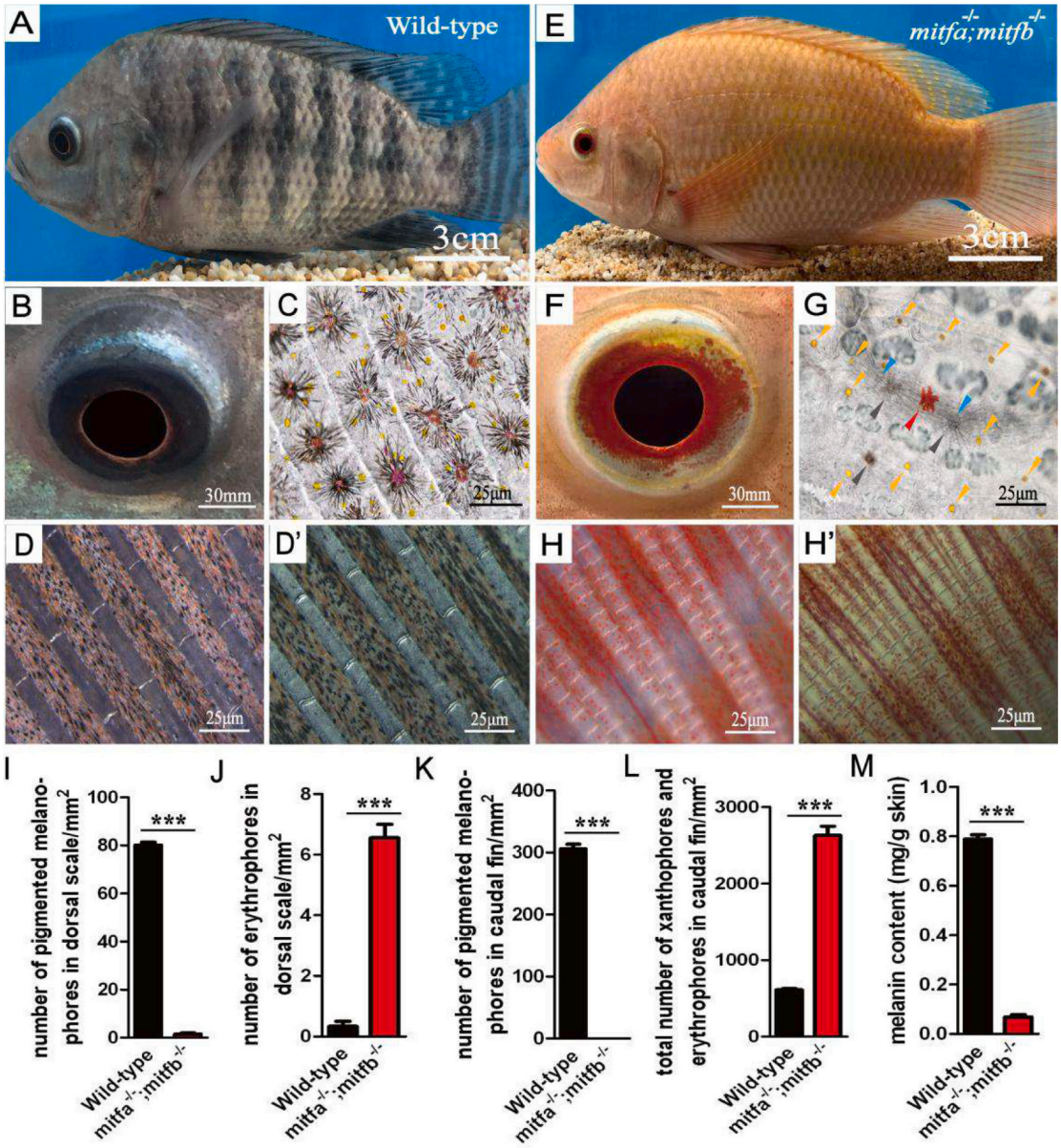

Fig. 6. Melanophores were significantly decreased, while erythrophores and xanthophores were significantly increased in *mitfa*$^{-/-}$;*mitfb*$^{-/-}$ mutants at 180 dpf. A, C, D, D′ and E: The wild-type fish displayed dark bars in the trunk and fins, and heavily pigmented RPE and iris. The caudal fin and scales were detected with many melanophores and xanthophores. B, F, G, G' and H: The *mitfa*$^{-/-}$;*mitfb*$^{-/-}$ mutants displayed dark red RPE and reddish-yellow body with no black bars in the trunk and fins due to hypo-pigmentation and increase of erythrophores (red arrow heads) and xanthophores (yellow arrow heads). The fins and scales were detected with significant increase of erythrophores, compared with the wild-type fish, and scales were detected with many xanthophores and some seriously hypo-pigmented melanophores with clusters. I, J: Quantitative analysis of the numbers of pigmented melanophores, erythrophores and xanthophores in the caudal fins of the mutants and wild-type fish. K, L: Quantitative analysis of the numbers of the fully pigmented melanophores and erythrophores in the dorsal scales of the mutants and wild-type fish. M: Quantification of the melanin content in the dorsal skin. Data in I-M are expressed as mean ± SD ($n = 5$). Differences in the data between the wild-type fish and mutants were tested by two-tailed Student's *t*-test, ***$P < 0.001$. (For interpretation of the references to color in this figure legend, the reader is referred to the web version of this article).

and accumulation of erythrophores. Most importantly, the sexually mature *mitfa*$^{-/-}$;*mitfb*$^{-/-}$ mutants had a very obvious red and yellow body color at 180 dpf, due to a vast increase in the number of erythrophores.

In general, the *mitfa*$^{-/-}$;*mitfb*$^{-/-}$ mutants displayed a phenotype similar to the red tilapia, a natural color mutant characterized by black RPE, significant decrease of or even absence of melanophores, significant increase of erythrophores and an accumulation of carotenoids-derived reddish pigmentation in iris (Avtalion and Reich, 1989; Hilsdorf et al., 2002; Wang et al., 2021a). Importantly, *mitf* was found to be down-regulated in red/white skin of red tilapia by skin transcriptome analysis (Zhu et al., 2016; Jiang et al., 2022a). Taken together, these results suggested a very close relationship between *mitf* genes and the red coloration. However, the color in red tilapia was mapped to a single "red" locus on linkage group 3 far from *mitfa* or *mitfb* (Lee et al., 2005). Therefore, we speculate that the promoter region of a *mitf*-regulated gene was mutated in red tilapia, and probably the "red" gene was transcriptionally regulated by Mitf.

Even though the *mitfa*$^{-/-}$;*mitfb*$^{-/-}$ mutants displayed red and yellow body color at the adult stage and appeared to have potential in the

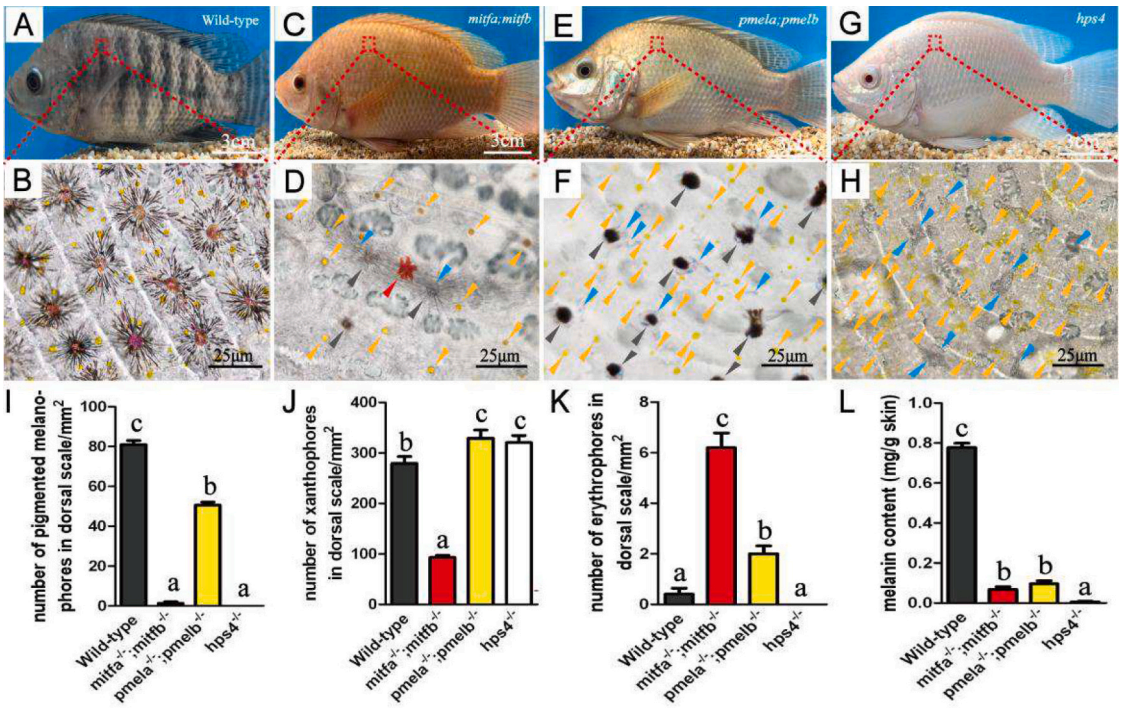

Fig. 7. Disruption of the three known classical melanogenesis genes conferred tilapia different body colors.
A, B: The wild-type fish displayed black coloration with vertical bars in trunk and median fins, and the dorsal scales were detected with many melanophores, many small round xanthophores, few erythrophores and many colorful iridophores. C, D: The *mitfa*$^{-/-}$;*mitfb*$^{-/-}$ mutants displayed red and yellow body color, and the dorsal scales were detected with a few hypo-pigmented melanophores with clusters (gray arrow heads), many large sized xanthophores (yellow arrow heads), increased erythrophores (red arrow head) and less colorful iridophores (blue arrow heads). E, F: The *pmela*$^{-/-}$;*pmelb*$^{-/-}$ mutants displayed golden body color, and the dorsal scales were detected with many large sized xanthophores (yellow arrow heads), a few small sized melanophores (black arrow heads) and many colorful iridophores (blue arrow heads). G: The *hps4*$^{-/-}$ mutants displayed a silver-white body color, and the dorsal scales were detected with no pigmented melanophores, many large sized xanthophores with dispersed pigments (yellow arrow heads) and many white iridophores (blue arrow heads) gathered as big round spots. I-L: Quantification of the pigmented melanophores, xanthophores, erythrophores and melanin content in the dorsal scales. Data are expressed as mean ± SD (n = 5), and are statistically evaluated by one-way ANOVA with Duncan's post hoc test. $P < 0.05$ was considered to be statistically significant, as indicated by different letters above the error bar. (For interpretation of the references to color in this figure legend, the reader is referred to the web version of this article).

aquaculture industry, the mechanisms responsible for this difference in pigmentation needs further investigation. Further analysis of skin transcriptomes, development of color patterning related to sex hormones, lineage analysis of erythrophores and xanthophores and analysis of the corresponding pigment metabolism (carotenoids and pteridines), are urgently needed.

4.2. Neither mitfa nor mitfb is necessary for RPE pigmentation in tilapia

Loss of function studies of *mitfa* have been reported in zebrafish, and *mitfa* has been shown to be fundamental for differentiation of NCCs into melanophore and iridophores (Lister et al., 1999; Lister et al., 2011; Petratou et al., 2018). The studies on *mitfb* mutation in zebrafish were focused on RPE development. Even though both *mitfa* and *mitfb* were found to be expressed in RPE, neither of them was found to be required for RPE development, as no significant changes of RPE development were detected in single or double mutants (Lister et al., 2001; Lane and Lister, 2012). To our knowledge, no loss of function studies of *mitfb* on body color pigmentation have been conducted. In this study, we generated *mitfb*$^{-/-}$ mutants in tilapia by CRISPR/Cas9. Significant hypo-pigmentation was detected in the yolk sac and whole embryo in early developmental stages, suggesting that *mitfb* is critical for embryonic pigmentation. Slight hypo-pigmentation, together with loose round black spots along the lateral line, were detected in the young *mitfb*$^{-/-}$ mutants. Besides, the melanophores in fins and scales were both significantly reduced compared with the wild-type fish, indicating that *mitfb* was also critical for melanophore differentiation, development and melanogenesis. The effects of *mitfb* on body color formation of tilapia turned out to be most important in embryonic stages, while less important in latter stages. Additionally, microphthalmia was observed in some of the *mitfb*$^{-/-}$ mutants and *mitfa*$^{-/-}$;*mitfb*$^{-/-}$ mutants, but never found in *mitfa*$^{-/-}$ mutants, suggesting sub-functionalization of *mitf* genes in tilapia after the third round of vertebrate genome duplication as suggested for *Xiphophorus* and zebrafish (Lister et al., 1999; Altschmied et al., 2002; Mellgren and Johnson, 2002). However, no microphthalmia has been observed in the latter two species.

Neither *mitfa* nor *mitfb* was responsible for RPE pigmentation in tilapia, which is consistent with studies in zebrafish (*mitfa* and *mitfb*) (Lane and Lister, 2012) and fighting fish (*mitfa*) (Wang et al., 2021b). The results from the three teleost species were absolutely different with those from human and mammals, in which disruption or natural allele mutation of *mitf* led to significant albinism, revealed by global hypo-pigmentation and even eye deficiency (as reflected by microphthalmia and hypo-pigmented RPE). These results indicate that *mitf* is not linked with RPE pigmentation in teleosts. How and why the *mitf* mutation led to different effects on RPE pigmentation and developmental effects between fishes and mammals still remains to be investigated.

Additionally, it should be not ignored that even though it is known that the functions of a gene are complex, and the color genes were often closely associated with the growth and physiological indicators of the mammals and other vertebrates (Hou and Pavan, 2008), so far, no evidence has shown that there were significant changes in growth or physiological indicators between the *mitf* mutants and the wild-type fish.

4.3. Modeling on the effects of mitf mutation on body color formation and pigment cells relative abundance

As the most well known and most important transcription factor in melanophore differentiation and melanogenesis, *mitf* has been associated with albinism, vitiligo, melanoma and other types of pigmentation disorders in human, mammals, birds, reptiles and teleosts. This gene was also closely linked to the economic trait of the domesticated animals including minks (Song et al., 2017), ducks (Zhou et al., 2018), and even fishes (Liu et al., 2016; Wang et al., 2021a), as people naturally associate particular body colors with beauty, health, and even food quality. In this study, we successfully conferred a red and yellow body color mutants in Nile tilapia by mutation of the *mitfa* and *mitfb* genes. The *mitfa*$^{-/-}$;*mitfb*$^{-/-}$ mutants showed serious hypo-pigmentation (Fig. 8A), with yellow body color and dispersed black spots at early juvenile stage (60 dpf), yellow-reddish body color at late juvenile stage (120 dpf) while an obvious red and yellow body color at adult stage (180 dpf). Phenotype analysis suggested that *mitf* genes were not only fundamental for melanophore survival, but also necessary for melanosome development and melanosome biosynthesis in tilapia.

Additionally, as a NCCs-pigment cell lineage marker gene, disruption of *mitf* also influences the relative abundance of the other types of pigment cells, similar to the results in zebrafish (Lister et al., 1999). However, there are some phenotypic differences due to the variance in the type and number of pigment cells and also color patterns of different fish species. Increased erythrophores (zebrafish has no erythrophores) and iridophores, and enlarged xanthophores were observed in the *mitfa*$^{-/-}$;*mitfb*$^{-/-}$ tilapia, which is the key reason for the red and yellow body color formation in adult fish (Fig. 8B). In our previous studies, Nile tilapia was found to have different mechanisms for color patterning compared with zebrafish. Tilapia have vertical bars and additional erythrophores, compared to the horizontal stripes and absence of erthyrophores in zebrafish (Wang et al., 2021a). The adult tilapia *mitfa*$^{-/-}$;*mitfb*$^{-/-}$ mutants can serve as an excellent model for revealing the mechanisms of erythrophore and xanthophore differentiation and their corresponding pigments (carotenoids and pteridines), which can be of great significance for understanding the basis of red coloration in teleosts.

4.4. Disruption of the three genes with different functions in different aspects of melanogenesis conferred different body colors

It seems that all roads in pigment diseases of human and mammals would finally lead to *mitf* (Hou and Pavan, 2008). Many genes in the *mitf*-axis (including downstream genes like *pmel* and *hps4*) are cis-regulated by this transcription factor. *Mitf* participates in the survival, migration and differentiation of melanoblast, melanophore development and melanin biosynthesis, while *pmel* and *hps4* are mainly involved in melanin biosynthesis. For more detail in melanin biosynthesis, MITF was necessary for melanosome development at all phases (phase I to phase IV); PMEL can form a fibrillar structure within the melanosome upon which melanin is deposited, the formation of PMEL fibrils

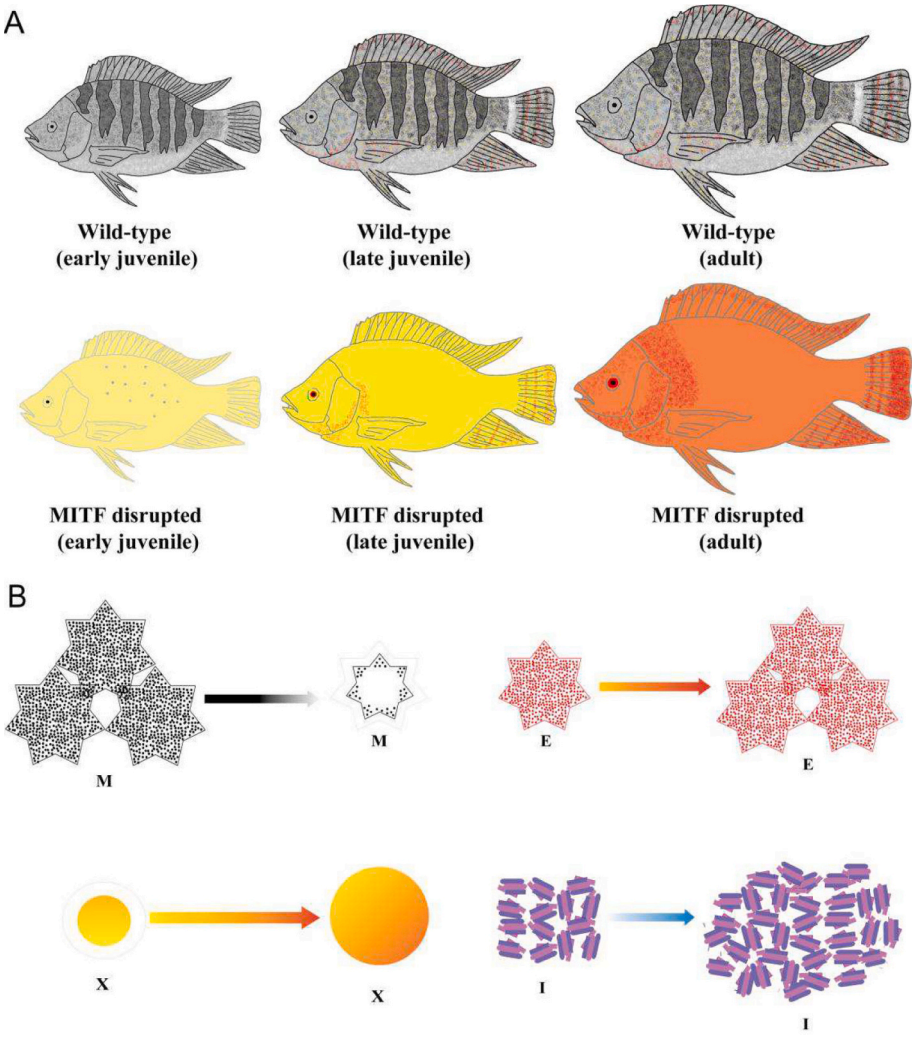

Fig. 8. Proposed model of MITF disruption in this study.
A: Disruption of *mitfa* and *mitfb* resulted in significant hypo-pigmentation in trunk and fins, yellow with black spots at early juvenile stage (60 dpf), yellow-reddish at late juvenile stage (120 dpf) and red and yellow with increasing red pigmentation in the body (including iris), especially at the end of the caudal fin and the joint of head and trunk at adult stage (180 dpf), but has no influence on RPE pigmentation. B: Disruption of *mitfa* and *mitfb* resulted in decreased and hypo-pigmented melanophores, increased erythrophores and iridophores and larger sized xanthophores. In addition to regulating melanophore differentiation and melanogenesis, this study demonstrated for the first time that *mitf* also participated in the lineage differentiation of erythrophores and xanthophores. M, melanophores; E, erythrophores; X, xanthophores; I, iridophores. (For interpretation of the references to color in this figure legend, the reader is referred to the web version of this article).

gradually converts phase I to phase II melanosomes (Yamaguchi and Hearing, 2009; Ito and Wakamatsu, 2011). While HPS4 is part of BLOC3 (biogenesis of lysosome-related organelles complex 3) which is involved in trafficking of melanosome cargo from the Golgi to stage III melanosomes (Wasmeier et al., 2008; Gerondopoulos et al., 2012). Both *pmel* and *hps4* have several *mitf* binding sites in their promoters, indicating the two genes are probably directly regulated by *mitf*. We have also successfully mutated *pmel* and *hps4* in tilapia (Wang et al., 2022a, 2022b). The *mitfa*$^{-/-}$;*mitfb*$^{-/-}$, *pmela*$^{-/-}$;*pmelb*$^{-/-}$ and *hps4*$^{-/-}$ mutants displayed different body colors which could be observed since early developmental stages, and became more obvious with development, especially in the adult stage.

The *pmela*$^{-/-}$;*pmelb*$^{-/-}$ mutants displayed golden color, with a few slow restored small-sized melanophores, but a great accumulation of xanthophores with significant larger sizes than in wild-type fish. As a comparison, the *hps4*$^{-/-}$ silver-white mutants were detected with significantly increased white iridophores than in wild-type fish, but with no pigmented melanophores. The *mitfa*$^{-/-}$;*mitfb*$^{-/-}$ mutants displayed red and yellow color, with the highest abundance of erythrophores, and with almost no pigmented melanophores in whole trunk and fins. Differences in the numbers and sizes of the pigment cells in the three color mutants suggests that disruption of the classic melanogenesis genes could confer different body colors. Most importantly, the adult *mitfa*$^{-/-}$;*mitfb*$^{-/-}$ mutants showed vast accumulation of erythrophores and large-sized xanthophores, which was completely different from the *pmela*$^{-/-}$;*pmelb*$^{-/-}$ and *hps4*$^{-/-}$ mutants. These results suggest that the increased number or area of erythrophores and xanthophores is probably due to the absence or reduction of melanophores in the mutants, as the change of neural crest cell fate specification revealed in studies (Kelsh et al., 2021).

It has been well documented that the upstream and downstream genes in *mitf* axis are down-regulated in the natural or induced melanin-reduced or melanin-absent color mutants in many fish species (Jiang et al., 2014; Zhu et al., 2016; Zhang et al., 2017a, 2017b; Wu et al., 2022; Liu et al., 2019). However, we did not perform skin transcriptome analysis, Western-blot or other follow-up analysis of the mutants. We speculate that the upstream and downstream genes in *mitf* axis were also down-regulated or silenced in our *mitf* mutants, as we detected few melanosomes in the skin of the red and yellow mutants (6 months) by melanin quantification analysis.

Traditional means to breed a stable color mutants were mainly conducted by cross-breeding with the closely-related fish species, or by selective breeding with the occasionally obtained natural color mutants, which were rather time-consuming. Gene editing as an efficient and powerful tool has been widely used to improve the economic traits in molecular breeding of animals and plants. The red and yellow tilapia, which we created by *mitf* double mutation, shows potential commercial value in aquaculture. However, China's current laws and consumer concerns hinder its current application. But we believe that this day will definitely come.

5. Conclusion

In conclusion, body color is an important economic trait of farmed fishes. In this study, we engineered a red and yellow tilapia by disrupting *mitfa* and *mitfb* with CRISPR/Cas9. Phenotype analysis confirmed that the *mitf* genes are critical for melanogenesis and melanophore survival, and *mitfb* was demonstrated to be also important for body color formation in tilapia by mutational analysis, even though it was less significant than *mitfa*. Both *mitfa*$^{-/-}$ and *mitfb*$^{-/-}$ mutants displayed black RPE throughout development, like the wild-type fish, indicating that neither *mitfa* nor *mitfb* was critical for RPE pigmentation in tilapia. Additionally, the adult *mitfa*$^{-/-}$;*mitfb*$^{-/-}$ mutants displayed a red and yellow body color due to significantly increased erythrophores and iridophores and significant enlarged xanthophores. These results suggested both sub-functionalization and neofunctionalization of *mitf* genes after duplication. To our knowledge, this is the first report on *mitf* genes being responsible for the number of erythrophores, size of xanthophores and involvement of *mitfb* in body color formation by loss of function studies. Our study provides not only an excellent model for studying *mitf* function in lower vertebrates, but also a new strategy for breeding red and yellow tilapia for aquaculture.

Supplementary data to this article can be found online at https://doi.org/10.1016/j.aquaculture.2022.739151.

Author contributions

DW acquired the funding, designed research, conducted investigation and administrated the project; CW created the mutants; TDK suggested strategies for phenotype analysis; CW, JW, PL, GL, BL, JX and XC participated in methology application and software analysis; CW and DW curated the data; CW, DW and TDK wrote the original draft; wrote, reviewed and edited the finalized manuscript.

Credit authorship contribution statement

Chenxu Wang: Software, Formal analysis, Validation, Data curation, Investigation, Resources, Writing – original draft, Writing – review & editing, Visualization. Thomas D. Kocher: Methodology, Writing – original draft, Writing – review & editing. Jinzhi Wu: Software, Formal analysis, Validation. Peng Li: Software, Formal analysis, Validation. Guangyuan Liang: Software, Formal analysis, Validation. Baoyue Lu: Software, Formal analysis, Validation. Jia Xu: Software, Formal analysis, Validation. Xiaoke Chen: Software, Formal analysis, Validation. Deshou Wang: Conceptualization, Investigation, Data curation, Writing – original draft, Writing – review & editing, Supervision, Project administration, Funding acquisition.

Declaration of Competing Interest

The authors declare that they have no known competing financial interests or personal relationships that could have appeared to influence the work reported in this paper.

Data availability

No data was used for the research described in the article.

Acknowledgements

This work was supported by grants 31872556, 31861123001 and 31630082 from the National Natural Science Foundation of China; grants cstc2021ycjh-bgzxm0024 and CQYC201903173 from the Chongqing Science and Technology Bureau and grants CYS17080 from the Chongqing Municipal Education Commission. We appreciate Prof. Jing Wei for her constant help in color patterning studies and her students Xiaoming Bai, Changle Zhao and Zhuo Yang for technical support and experimental fish caring. We also would like to thank Prof. Ling Hou and his group from Wenzhou Medical University for providing references.

References

Altschmied, J., Delfgaauw, J., Wilde, B., Duschl, J., Bouneau, L., Volff, J.N., et al., 2002. Subfunctionalization of duplicate *mitf* genes associated with differential degeneration of alternative exons in fish. Genetics 161 (1), 259–267.

Avtalion, R.R., Reich, L., 1989. Chromatophore inheritance in red tilapias. The Isr. J. Aquacult-Bamid. 41 (3), 98–104.

Béjar, J., Hong, Y., Schartl, M., 2003. *Mitf* expression is sufficient to direct differentiation of medaka blastula derived stem cells to melanocytes. Development 130 (26), 6545–6553.

Braasch, I., Brunet, F., Volff, J.N., Schartl, M., 2009. Pigmentation pathway evolution after whole-genome duplication in fish. Genome. Biol. Evol. 7, 479–493.

Cheli, Y., Ohanna, M., Ballotti, R., Bertolotto, C., 2010. Fifteen-year quest for microphthalmia-associated transcription factor target genes. Pigment Cell Melan. Res. 23 (1), 27–40.
Frohnhöfer, H.G., Krauss, J., Maischein, H.M., Nüsslein-Volhard, C., 2013. Iridophores and their interactions with other chromatophores are required for stripe formation in zebrafish. Development 140 (14), 2997–3007.
Fujii, R., 2000. The regulation of motile activity in fish chromatophores. Pigment Cell Res. 13 (5), 300–319.
Fukamachi, S., Sugimoto, M., Mitani, H., Shima, A., 2004. Somatolactin selectively regulates proliferation and morphogenesis of neural-crest derived pigment cells in medaka. Proc. Natl. Acad. Sci. U. S. A. 101 (29), 10661–10666.
George, A., Zand, D.J., Hufnagel, R.B., Sharma, R., Sergeev, Y.V., Legare, J.M., et al., 2016. Biallelic mutations in MITF cause coloboma, osteopetrosis, microphthalmia, macrocephaly, albinism, and deafness. Am. J. Hum. Genet. 99 (6), 1388–1394.
Gerondopoulos, A., Langemeyer, L., Liang, J.R., Linford, A., Barr, F.A., 2012. BLOC-3 mutated in Hermansky–Pudlak syndrome is a Rab32/38 guanine nucleotide exchange factor. Curr. Biol. 22, 2135–2139.
Goding, C.R., Arnheiter, H., 2019. MITF-the first 25 years. Genes Dev. 33 (15–16), 983–1007.
Hai, T., Guo, W., Yao, J., Cao, C., Luo, A., Qi, M., et al., 2017. Creation of miniature pig model of human Waardenburg syndrome type 2A by ENU mutagenesis. Hum. Genet. 136 (11–12), 1463–1475.
Hilsdorf, A.W., Penman, D.J., Farias, E.C., McAndrew, B., 2002. Melanophore appearance in wild and red tilapia embryos. Pigment Cell Res. 15 (1), 57–61.
Hodgkinson, C.A., Moore, K.J., Nakayama, A., Steingrímsson, E., Copeland, N.G., Jenkins, N.A., et al., 1993. Mutations at the mouse microphthalmia locus are associated with defects in a gene encoding a novel basic-helix-loop-helix-zipper protein. Cell 74 (2), 395–404.
Hoekstra, H.E., 2006. Genetics, development and evolution of adaptive pigmentation in vertebrates. Heredity (Edinb) 97 (3), 222–234.
Hofreiter, M., Schöneberg, T., 2010. The genetic and evolutionary basis of colour variation in vertebrates. Cell. Mol. Life Sci. 67 (15), 2591–2603.
Hou, L., Pavan, W.J., 2008. Transcriptional and signaling regulation in neural crest stem cell-derived melanocyte development: do all roads lead to *Mitf*? Cell Res. 18 (12), 1163–1176.
Hubbard, J.K., Uy, J.A., Hauber, M.E., Hoekstra, H.E., Safran, R.J., 2010. Vertebrate pigmentation: from underlying genes to adaptive function. Trends Genet. 26 (5), 231–239.
Ito, S., Wakamatsu, K., 2011. Human hair melanins: what we have learned and have not learned from mouse coat color pigmentation. Pigment Cell Melanoma Res. 24 (1), 63–74.
Jiang, Y., Zhang, S., Xu, J., Feng, J., Mahboob, S., Al-Ghanim, K.A., et al., 2014. Comparative transcriptome analysis reveals the genetic basis of skin color variation in common carp. PLoS One 9 (9), e108200.
Jiang, B., Wang, L., Luo, M., Fu, J., Zhu, W., Liu, W., et al., 2022a. Transcriptome analysis of skin color variation during and after overwintering of Malaysian red tilapia. Fish Physiol. Biochem. 48 (3), 669–682.
Jiang, B., Wang, L., Luo, M., Zhu, W., Fu, J., Dong, Z., 2022b. Molecular and functional analysis of the microphthalmia-associated transcription factor (*mitf*) gene duplicates in red tilapia. Comp. Biochem. Physiol. A Mol. Integr. Physiol. 271, 111257.
Kawasaki, A., Kumasaka, M., Satoh, A., Suzuki, M., Tamura, K., Goto, T., et al., 2008. *Mitf* contributes to melanosome distribution and melanophore dendricity. Pigment Cell Melan. Res. 21 (1), 56–62.
Kelsh, R.N., 2004. Genetics and evolution of pigment patterns in fish. Pigment Cell Res. 17 (4), 326–336.
Kelsh, R.N., Sosa, K.C., Farjami, S., Makeev, V., Dawes, J.H.P., Rocco, A., 2021. Cyclical fate restriction: a new view of neural crest cell fate specification. Development 148 (22), dev176057.
Kimura, T., Nagao, Y., Hashimoto, H., Yamamoto-Shiraishi, Y., Yamamoto, S., Yabe, T., et al., 2014. Leucophores are similar to xanthophores in their specification and differentiation processes in medaka. Proc. Natl. Acad. Sci. U. S. A. 111 (20), 7343–7348.
Körberg, I.B., Sundström, E., Meadows, J.R.S., Pielberg, G.R., Gustafson, U., Hedhammar, Å., et al., 2014. A simple repeat polymorphism in the MITF-M promoter is a key regulator of white spotting in dogs. PLoS One 9, e104363.
Lane, B.M., Lister, J.A., 2012. *Otx* but not *Mitf* transcription factors are required for zebrafish retinal pigment epithelium development. PLoS One 7 (11), e49357.
Lee, B.Y., Lee, W.J., Streelman, J.T., Carleton, K.L., Howe, A.E., Hulata, G., et al., 2005. A second-generation genetic linkage map of tilapia (*Oreochromis spp.*). Genetics 170 (1), 237–244.
Levy, C., Khaled, M., Fisher, D.E., 2006. MITF: master regulator of melanocyte development and melanoma oncogene. Trends Mol. Med. 12 (9), 406–414.
Li, M., Zhu, F., Hong, N., Zhang, L., Hong, Y., 2014. Alternative transcription generates multiple *Mitf* isoforms with different expression patterns and activities in medaka. Pigment Cell Melan. Res. 27 (1), 48–58.
Lister, J.A., Robertson, C.P., Lepage, T., Johnson, S.L., Raible, D.W., 1999. *nacre* encodes a zebrafish microphthalmia-related protein that regulates neural-crest-derived pigment cell fate. Development 126 (17), 3757–3767.
Lister, J.A., Close, J., Raible, D.W., 2001. Duplicate *mitf* genes in zebrafish: complementary expression and conservation of melanogenic potential. Dev. Biol. 237 (2), 333–344.
Lister, J.A., Lane, B.M., Nguyen, A., Lunney, K., 2011. Embryonic expression of zebrafish MiT family genes *tfe3b*, *tfeb*, and *tfec*. Dev. Dyn. 240 (11), 2529–2538.
Liu, J.H., Wen, S., Luo, C., Zhang, Y.Q., Tao, M., Wang, D.W., et al., 2016. Involvement of the *mitfa* gene in the development of pigment cell in Japanese ornamental (koi) carp (*Cyprinus carpio L.*). Genet. Mol. Res. 14 (1), 2775–2784.
Liu, Q., Qi, Y., Liang, Q., Song, J., Liu, J., Li, W., et al., 2019. Targeted disruption of tyrosinase causes melanin reduction in *Carassius auratus cuvieri* and its hybrid progeny. Sci. China Life Sci. 62 (9), 1194–1202.
Lopes, S.S., Yang, X., Müller, J., Carney, T.J., McAdow, A.R., Rauch, G.J., et al., 2008. Leukocyte tyrosine kinase functions in pigment cell development. PLoS Genet. 4 (3), e1000026.
Lorin, T., Brunet, F.G., Laudet, V., Volff, J.N., 2018. Teleost fish-specific preferential retention of pigmentation gene-containing families after whole genome duplications in vertebrates. G3-Genes Genom. Genet. (Bethesda) 8 (5), 1795–1806.
Mellgren, E.M., Johnson, S.L., 2002. The evolution of morphological complexity in zebrafish stripes. Trends Genet. 18 (3), 128–134.
Mort, R.L., Jackson, I.J., Patton, E.E., 2015. The melanocyte lineage in development and disease. Development 142 (4), 620–632.
Parichy, D.M., 2007. Homology and the evolution of novelty during Danio adult pigment pattern development. J. Exp. Zool. B Mol. Dev. Evol. 308 (5), 578–590.
Petratou, K., Subkhankulova, T., Lister, J.A., Rocco, A., Schwetlick, H., Kelsh, R.N., 2018. A systems biology approach uncovers the core gene regulatory network governing iridophore fate choice from the neural crest. PLoS Genet. 14 (10), e1007402.
Salis, P., Lorin, T., Laudet, V., Frédérich, B., 2019. Magic traits in magic fish: understanding color pattern evolution using reef fish. Trends Genet. 35 (4), 265–278.
Schneider, C.A., Rasband, W.S., Eliceiri, K.W., 2012. NIH image to ImageJ: 25 years of image analysis. Nat. Methods 9 (7), 671–675.
Singh, A.P., Nüsslein-Volhard, C., 2015. Zebrafish stripes as a model for vertebrate colour pattern formation. Curr. Biol. 25 (2), R81–R92.
Sköld, H.N., Aspengren, S., Cheney, K.L., Wallin, M., 2016. Fish chromatophores-from molecular motors to animal behavior. Int. Rev. Cell Mol. Biol. 321, 171–219.
Song, X., Xu, C., Liu, Z., Yue, Z., Liu, L., Yang, T., et al., 2017. Comparative transcriptome analysis of mink (*Neovison vison*) skin reveals the key genes involved in the melanogenesis of black and white coat colour. Sci. Rep. 7 (1), 12461.
Sugimoto, M., 2002. Morphological color changes in fish: regulation of pigment cell density and morphology. Microsc. Res. Tech. 58 (6), 496–503.
Sun, Y.L., Jiang, D.N., Zeng, S., Hu, C.J., Ye, K., Yang, C., et al., 2014. Screening and characterization of sex-linked DNA markers and marker-assisted selection in the Nile tilapia (*Oreochromis niloticus*). Aquaculture 433, 19–27.
Taylor, K.L., Lister, J.A., Zeng, Z., Ishizaki, H., Anderson, C., Kelsh, R.N., et al., 2011. Differentiated melanocyte cell division occurs in vivo and is promoted by mutations in *Mitf*. Development 138 (16), 3579–3589.
Vachtenheim, J., Borovanský, J., 2010. "transcription physiology" of pigment formation in melanocytes: central role of MITF. Exp. Dermatol. 19 (7), 617–627.
Wang, X., Zhou, J., Cao, C., Huang, J., Hai, T., Wang, Y., et al., 2015. Efficient CRISPR/Cas9-mediated biallelic gene disruption and site-specific knockin after rapid selection of highly active sgRNAs in pigs. Sci. Rep. 5, 13348.
Wang, C., Lu, B., Li, T., Liang, G., Xu, M., Liu, X., et al., 2021a. Nile tilapia: a model for studying teleost color patterns. J. Hered. 112 (5), 469–484.
Wang, L., Sun, F., Wan, Z.Y., Ye, B., Wen, Y., Liu, H., et al., 2021b. Genomic basis of striking fin shapes and colors in the fighting fish. Mol. Biol. Evol. 38 (8), 3383–3396.
Wang, C., Xu, J., Kocher, T.D., Li, M., Wang, D., 2022a. CRISPR knockouts of *pmela* and *pmelb* engineered a golden tilapia by regulating relative pigment cell abundance. J. Hered. 113 (4), 398–413.
Wang, C., Kocher, T.D., Lu, B., Xu, J., Wang, D., 2022b. Knockout of Hermansky-Pudlak Syndrome 4 (*hps4*) leads to silver-white tilapia lacking melanosomes. Aquaculture 738420. Online ahead of print.
Wasmeier, C., Hume, A.N., Bolasco, G., Seabra, M.C., 2008. Melanosomes at a glance. J. Cell Sci. 121, 3995–3999.
Wu, S., Huang, J., Li, Y., Zhao, L., Liu, Z., 2022. Analysis of yellow mutant rainbow trout transcriptomes at different developmental stages reveals dynamic regulation of skin pigmentation genes. Sci. Rep. 12 (1), 256.
Yamaguchi, Y., Hearing, V.J., 2009. Physiological factors that regulate skin pigmentation. Biofactors 35 (2), 193–199.
Zhang, Y., Liu, J., Fu, W., Xu, W., Zhang, H., Chen, S., et al., 2017a. Comparative transcriptome and DNA methylation analyses of the molecular mechanisms underlying skin color variations in crucian carp (*Carassius carassius L.*). BMC Genet. 18, 95.
Zhang, Y., Liu, J., Peng, L., Ren, L., Zhang, H., Zou, L., et al., 2017b. Comparative transcriptome analysis of molecular mechanism underlying gray-to-red body color formation in red crucian carp (*Carassius auratus, red var.*). Fish Physiol. Biochem. 43 (5), 1387–1398.
Zhou, Z., Li, M., Cheng, H., Fan, W., Yuan, Z., Gao, Q., et al., 2018. An intercross population study reveals genes associated with body size and plumage color in ducks. Nat. Commun. 9 (1), 3974.
Zhu, W., Wang, L., Dong, Z., Chen, X., Song, F., Liu, N., et al., 2016. Comparative transcriptome analysis identifies candidate genes related to skin color differentiation in red tilapia. Sci. Rep. 6, 31347.